Biochimica et Biophysica Acta 1837 (2014) 908–919

Contents lists available at ScienceDirect

Biochimica et Biophysica Acta

journal homepage: www.elsevier.com/locate/bbabio

The role of the high potential form of the cytochrome *b*559: Study of *Thermosynechococcus elongatus* mutants

Fernando Guerrero [a,b,1], Jorge L. Zurita [a,b,2], Mercedes Roncel [a], Diana Kirilovsky [b], José M. Ortega [a,*]

[a] Instituto de Bioquímica Vegetal y Fotosíntesis, Universidad de Sevilla-CSIC, Américo Vespucio 49, 41092 Seville, Spain
[b] Laboratoire de Bioénergétique Moléculaire et Photosynthèse, Institut de Biologie et de Technologies de Saclay (iBiTec-S), CEA Saclay, 91191 Gif-sur-Yvette cedex, France

ARTICLE INFO

Article history:
Received 30 October 2013
Received in revised form 21 February 2014
Accepted 26 February 2014
Available online 5 March 2014

Keywords:
Cytochrome *b*559
High potential form
Photosystem II
Redox potentiometry
Site-directed mutagenesis
Thermosynechococcus elongatus

ABSTRACT

Cytochrome *b*559 is an essential component of the photosystem II reaction center in photosynthetic oxygen-evolving organisms, but its function still remains unclear. The use of photosystem II preparations from *Thermosynechococcus elongatus* of high integrity and activity allowed us to measure for the first time the influence of cytochrome *b*559 mutations on its midpoint redox potential and on the reduction of the cytochrome *b*559 by the plastoquinone pool (or Q_B). In this work, five mutants having a mutation in the α-subunit (I14A, I14S, R18S, I27A and I27T) and one in the β-subunit (F32Y) of cytochrome *b*559 have been investigated. All the mutations led to a destabilization of the high potential form of the cytochrome *b*559. The midpoint redox potential of the high potential form was significantly altered in the αR18S and αI27T mutant strains. The αR18S strain also showed a high sensitivity to photoinhibitory illumination and an altered oxidase activity. This was suggested by measurements of light induced oxidation and dark re-reduction of the cytochrome *b*559 showing that under conditions of a non-functional water oxidation system, once the cytochrome is oxidized by $P680^+$, the yield of its reduction by Q_B or the PQ pool was smaller and the kinetic slower in the αR18S mutant than in the wild-type strain. Thus, the extremely positive redox potential of the high potential form of cytochrome *b*559 could be necessary to ensure efficient oxidation of the PQ pool and to function as an electron reservoir replacing the water oxidation system when it is not operating.

1. Introduction

In higher plants, algae and cyanobacteria, the primary steps of photosynthetic light conversion take place in a large pigment–protein complex named photosystem II (PSII), which drives light-induced electron transfer from water to plastoquinone (PQ) with the concomitant production of molecular oxygen (for a review see [1]). The reaction center (RC) of PSII is composed of an heterodimer formed by the D1 and D2 membrane proteins that bears all the cofactors needed for charge separation and stabilization: six chlorophylls (Chl) (including four of the Chl center, P680), two pheophytins, two plastoquinones Q_A and Q_B, one non-heme iron atom, one tetranuclear manganese cluster (Mn_4CaO_5) and two redox active tyrosines. A hemeprotein, named cytochrome *b*559 (Cyt *b*559), appears also tightly bound to RC in all photosynthetic oxygen-evolving organisms.

Cyt *b*559 is one of the essential components of PSII RC, but its function although widely investigated, still remains unclear (for a review see [2,3]). The resolution of the 3-D structure of PSII has clearly established that Cyt *b*559 is a heme-bridged protein heterodimer with two subunits (α and β, encoded by *psbE* and *psbF* genes) of 9 and 4 kDa, respectively [4–7]. Each polypeptide chain forms a transmembrane α-helix, the heme being located near the stromal side and perpendicular to the membrane plane. A bis-histidine axial coordination for the heme is largely supported by these structural studies.

Cyt *b*559 is a *b*-type cytochrome with peculiar physicochemical properties. It is found in PSII preparations in three different states: a high potential form (HP) with a midpoint redox potential (E_m) of ≈ +400 mV, another intermediate potential form (IP) with an E_m of ≈ +200 mV and a low potential form (LP) whose E_m ranges from +80 and 0 mV depending on the organisms [3,8–12]. Many authors have proposed that the HP

Abbreviations: B band, thermoluminescence emission due to $S_{2/3}Q_B^-$ charge recombination reaction; Chl, chlorophyll; Cm, chloramphenicol; CP43, a proximal antenna complex of photosystem II; Cyt, cytochrome; E_h, redox potential of the solution; E_m, midpoint redox potential; HP, IP and LP, high, intermediate and low potential forms; HTL, high temperature thermoluminescence; MES, 2-(N-morpholino) ethanesulfonic acid; OEC, oxygen evolving complex; P680, primary electron donor in PSII; PSII, photosystem II; Q_A and Q_B, the primary and secondary quinone acceptors of the reaction center of PSII; RC, reaction center; S_2 and S_3, oxidized states of the manganese oxygen-evolving complex of PSII; Sm, streptomycin; Sp, spectinomycin; TL, thermoluminescence

* Corresponding author. Tel.: +34 954489573; fax: +34 954460065.
E-mail addresses: Fernando.guerrero@helsinki.fi (F. Guerrero), jorge.zurita@juntadeandalucia.es (J.L. Zurita), mroncel@us.es (M. Roncel), kirilovsky@cea.fr (D. Kirilovsky), ortega@us.es (J.M. Ortega).
[1] Present address: Institute of Biotechnology, University of Helsinki, Viikinkaari 1, 00014 Helsinki, Finland.
[2] Present address: Fundación Progreso y Salud, Junta de Andalucía, Américo Vespucio 5, 41092 Seville, Spain.

http://dx.doi.org/10.1016/j.bbabio.2014.02.024
0005-2728/

form is the physiological and functional state of Cyt *b*559 [3,10]. However, the HP form is labile and easily converted to the LP/IP forms by treatments that alter the membrane structure or during the process of PSII isolation [8,10]. In plants, algae and cyanobacteria, different kinds of PSII preparations with very variable percentages of the HP form, peaking at about 80% have been described [8,10,11,13,14].

A great number of hypotheses have been put forth in order to explain the function of Cyt *b*559. Most of them propose that this protein may participate in secondary electron transfer pathways protecting PSII against oxidative damage [15–18]. In these proposals, Cyt *b*559 would donate electrons, via a β-carotene molecule, to reduce highly oxidizing chlorophyll radicals generated in PSII RC under donor-side photoinhibitory conditions [17,19,20]. On the other hand, Cyt *b*559 may accept electrons from the acceptor side of PSII (Q_B or PQ) to prevent the formation of damaging singlet oxygen species under acceptor-side photoinhibitory conditions [8,21,22].

Different new roles as oxygen reductase, superoxide reductase, superoxide oxidase and plastoquinol oxidase have been recently proposed for Cyt *b*559 [12,22–25]. The role as plastoquinol oxidase, taking electrons from the plastoquinone pool, has been supported by the existence of a third quinone, Q_C, different from the quinone sites, Q_A and Q_B, at 15 Å only from the heme of Cyt *b*559 [7]. Some authors have postulated the existence of three quinones, besides Q_A, in PSII core complex preparations of *Thermosynechococcus (T.) elongatus* [26,27]. A function for Q_C associated with a secondary electron transfer along the Cyt *b*559 in PSII has been proposed by Guskov et al. [7]. Therefore, a role for Cyt *b*559 as part of a connecting channel between the plastoquinone pool and Q_B and Q_C sites would be possible.

Most of the site-directed mutagenesis studies of the α- and β-subunits of Cyt *b*559 have been carried out in *Chlamydomonas reinhardtii* and *Synechocystis* sp. PCC 6803. No stable PSII was assembled when the heme-coordinating histidines were replaced by leucines [28], neither when the histidine of the α-subunit was replaced by tyrosine or methionine [29], or in deletion mutants of the α-subunit [30] and of both α- and β-subunits [31]. In fact, all these mutants were impaired in the functional PSII assembly and therefore not useful for determining the function of Cyt *b*559 in PSII.

Recently, a set of site-directed mutants of Cyt *b*559 in *Synechocystis* sp. PCC 6803 that grew photoautotrophically and accumulated stable PSII RC's has been constructed [14,32,33]. Mutants with changes on heme coordination (His22 of the α- or β-subunit) and on charged residues of the cytoplasmic side of Cyt *b*559 (R7Eα, R17Eα and R17Lβ) showed a higher sensitivity to photoinhibition than the WT strain. These results have led the authors to propose a functional role of Cyt *b*559 in protection of PSII under photoinhibition conditions [14]. They also suggested that the electrostatic interactions between these arginine residues and the heme propionates of Cyt *b*559 are essential in the maintenance of the structure and redox properties of the cytochrome. However, the *Synechocystis* sp. PCC 6803 strain used in this work seems to present an important limitation for the study of the Cyt *b*559 role because the PSII preparations contained very low proportions of the HP form [14,33].

The thermophilic cyanobacterium *T. elongatus* has become in the last years a new model organism for photosynthesis researches, since genetic engineering techniques have been developed [34,35] and several 3-D structures of PSII have been solved from it [4,6,7,36]. In 2003, our group was already able to obtain PSII preparations from *T. elongatus*, 50% containing the HP form of cytochrome *b*559 and 50% an IP form, both in their reduced state [11]. No LP form was present in these preparations. The HP form in *T. elongatus* showed the typical redox properties of the HP form in higher plants: (1) it has a highly oxidizing E_m, which is not affected by pH [11] and (2) it is partially converted into a form of lower potential (IP) by treatments such as washing with Tris or gentle heating [11]. Recently, PSII preparations with a higher degree of integrity and activity have been prepared in our groups using a new His-tagged CP43 *T. elongatus* strain ([37] and this work). This is essential to study the properties of the Cyt *b*559 HP form. The high rates of O_2 evolution obtained in these preparations were good indicators of the integrity of the donor side of PSII ([37] and Table 1). The 1:1 ratio of the concentration of Cyt *b*559 regarding Cyt *c*550 [37] indicates that Cyt *c*550 is not released from PSII during the isolation process, also a good indicator of donor side integrity. The most important characteristic of these isolated PSII complexes is that 85% of them presented Cyt *b*559 in the reduced HP form with an E_m value of about +400 mV. Thus, our PSII preparations are an excellent material for the study of the effect of changes in the E_m values and on the percentage of HP/IP forms on the function of Cyt *b*559.

A series of site-directed mutants of Cyt *b*559, each carrying a single amino acid substitution, has been constructed in the thermophilic cyanobacterium *T. elongatus*, in order to modify the redox potential of the heme without altering the assembly properties of PSII. In this work we have analyzed in depth six of these mutant strains: five in the α-subunit (I14A, I14S, R18S, I27A and I27T) and one in the β-subunit (F32Y). All mutants grew photoautotrophically and assembled functionally PSII RC. For the first time, the redox potential of site-directed mutants of Cyt *b*559 has been determined. The E_m of the HP form of Cyt *b*559 was significantly altered in two of the mutant strains: αR18S and αI27T. The αR18S strain also showed a high sensitivity to photoinhibitory illumination. The results support the proposal that the HP form of Cyt *b*559 may function in a secondary electron transfer cycle in order to protect PSII when the water oxidation system is impaired.

2. Material and methods

2.1. Construction of plasmids for the mutation of cytochrome b559

The genome region containing the genes *psbE*, *psbF*, *psbL* and *psbJ* (forming an operon) (Fig. 1) was amplified by PCR using the oligonucleotides *cytb559BssHIIa* and *cytb559BssHIIb* (Supplementary Table I). The amplified region which includes part of the *tlr1540* gene encoding a serine–threonine kinase was digested by BssHII and cloned. The *tlr1540* gene was interrupted by insertion of a 2.2 kb DNA fragment containing the *aadA* gene from Tn7, conferring resistance to spectinomycin (Sp) and streptomycin (Sm) [38], in the unique KpnI restriction site of the *tlr1540* gene. Site-directed mutagenesis of the plasmid containing the interrupted *tlr1540* gene was performed using the QuikChange XL site-directed mutagenesis kit of Stratagene as recommended by the manufacturer. The synthetic mutagenic oligonucleotides used to create the different point mutations in the *psbE* and *psbF* genes (encoding for the α and β-subunits of the Cyt *b*559, respectively) are shown in Supplementary Table II. The mutagenic oligonucleotides also introduced a silent mutation creating or eliminating restriction enzyme sites for mutant screening.

2.2. Transformation of T. elongatus cells and genetic analysis of mutants

The construction of WT' strain of *T. elongatus*, containing a His-tagged CP43 for isolation of PSII complexes with high activity, was described in Guerrero et al. [37]. The plasmids containing the site-mutated *psbE* and *psbF* genes were introduced in WT' by electroporation according to Mühlenhoff and Chauvat [34] with slight modifications as described in [39]. To create the control strain WT", a plasmid containing the *psbE* and *psbF* genes (without mutations) and the *tlr1540* gene interrupted by the Sp/Sm resistance cassette was introduced into WT' cells.

After electroporation, cells were rapidly transferred to 2 ml of DTN-medium [34] and incubated for 48 h in a rotary incubator at 45 °C under low light conditions. Then, the cells in 0.1–0.2 ml aliquots were spread on plates containing chloramphenicol (Cm) (2 μg ml^{-1}) or Sp/Sm (12 μg ml^{-1}/6 μg ml^{-1}) and incubated at 45 °C, under dim light and a humidified atmosphere. Once green

Table 1
Potentiometric redox characterization of cytochrome *b*559 and oxygen evolution activity in PSII preparations from *Thermosynechococcus elongatus* wild-type and cytochrome *b*559 site-directed mutants. The values for the midpoint redox potential (E_m) and percentages (%) of the HP and IP forms of cytochrome *b*559 are the average values of six independent experiments. The error in the determination of E_m (standard deviation, STD) is also indicated. The oxygen evolution activities in PSII preparations and in whole cells are also indicated.

Strain	E_m (mV) (mean, STD)		%		Oxygen evolution (μmol O_2 mg Chl^{-1} h^{-1})	
	HP	IP	HP	IP	PSII	cells
WT"	+394 ± 3	+240 ± 11	85	15	3240	249
αI14A	+370 ± 13	+210 ± 15	55	45	2510	239
αI14S	+366 ± 16	+218 ± 14	55	45	2370	233
αR18S	+330 ± 9	+210 ± 10	68	32	2507	232
αI27A	+353 ± 12	+210 ± 7	56	44	2520	242
αI27T	+308 ± 11	+208 ± 9	70	30	2450	236
βF32Y	+361 ± 8	+241 ± 7	74	26	2310	248

colonies appeared (2–3 weeks), they were spread at least twice on agar plates containing Cm (5 μg ml^{-1}) or Sp/Sm (25 μg ml^{-1}/10 μg ml^{-1}) before their genomic DNA was analyzed. Genomic DNA was isolated from *T. elongatus* cells essentially as described by Cai and Wolk [40]. To confirm the homoplasmicity of the mutants, PCR analysis were carried out using different primers (Supplementary Tables I and II). To verify that the desired point mutations were present in the transformed *T. elongatus* cells, PCR amplified fragments of 3.3 kb containing the *psbE* and *psbF* genes were obtained using the oligonucleotides *Cytb559a'* and *PsbJ + 76rev* or *SpSmAntisense* and *psbJ + 76rev* (Supplementary Table I). The fact that a 1.2 kb PCR fragment was not detected in these mutants indicated that complete segregation and total homoplasmicity were achieved. Since the double recombination could occur between the antibiotic cassette and the point mutations, not all of the Sp/Sm resistant mutants contained the site-directed mutations. To select the mutants carrying the proper modified bases, the 3.3 kb amplified fragment was checked by digestion with the different restriction enzymes depending on the mutation. The presence of the mutations was also checked for some mutants by amplifying a DNA fragment with the oligonucleotides *SpSmAntisense* and *psbJ + 76rev*. The amplified DNA fragment of 1.34 kb was then digested by different restriction enzymes. The mutant PCR fragments were then sequenced to confirm that the correct mutation was the only modification present in the gene. The PCR analyses were regularly repeated to verify the genotype in the cells used for phenotype characterization.

2.3. Standard culture conditions

Cells of all the strains of *T. elongatus* were grown in a DTN-medium [34] with a CO_2-enriched atmosphere (1%) in a rotary shaker (120 rpm) at 45 °C. Continuous illumination was provided by fluorescent white lamps giving an intensity of 40 μE m^{-2} s^{-1}. For maintenance, the WT' mutant cells were grown in the presence of Cm (5 μg ml^{-1}) and the WT" and Cyt *b*559 mutant cells in the presence of Sp/Sm (25 μg ml^{-1}/10 μg ml^{-1}). To obtain PSII preparations, the cells were grown in 3-liter conical flasks (1500 ml culture). For growth rate and photoinhibition experiments, WT" and Cyt *b*559 mutant cells were grown in a DTN-medium agitated by the bubbling of a CO_2-enriched atmosphere (1%) using "bottles" (out of incubators) immersed in a water bath at 45 °C. The cultures were illuminated continuously with white light (100 or 700 μE m^{-2} s^{-1}).

2.4. Photosystem II core complex preparation

PSII core complexes were prepared from cells of *T. elongatus* by nickel affinity chromatography as described by Kirilovsky et al. [39]. The PSII core complex preparations were suspended in 40 mM MES, pH 6.5, 15 mM $CaCl_2$, 15 mM $MgCl_2$, 10% glycerol and 1 M glycinebetaine at about 2–3 mg Chl ml^{-1} and stored in liquid N_2. The preparations used in this work had an oxygen evolution activity of 2300–3200 μmol O_2 mg Chl^{-1} h^{-1} and contain Cyt *b*559 mostly in its reduced state in WT and all mutant strains investigated (data not shown; see Supplementary Fig. 1 and references [11] and [37]).

2.5. Oxygen evolution measurements

Oxygen evolution was measured at 25 °C by polarography using a Clark-type oxygen electrode (Hansatech) with saturating and continuous white light (10,000 μE m^{-2} s^{-1}). Oxygen evolution was measured in 40 mM Mes pH 6.5, 15 mM $MgCl_2$, 15 mM $CaCl_2$ at 5 μg Chl ml^{-1} for PSII core complexes and 10 μg Chl ml^{-1} for cells, and in the presence of 0.5 or 1 mM DCBQ (2,6-dichloro-*p*-benzoquinone) respectively, as electron acceptor.

2.6. Redox potential measurements

Potentiometric redox titrations were carried out basically as described in Guerrero et al. [37]. For titrations, samples containing PSII core complexes (30–50 μg Chl ml^{-1}) were suspended in 2.5-ml buffer containing 50 mM MES, pH 6.5. A set of the following eight redox mediators was added: 10 μM *p*-benzoquinone (E_{m7} = +280 mV), 20 μM 2,3,5,6-tetramethyl-*p*-phenylendiamine (also called diaminodurol or DAD) (E_{m7} = +220 mV), 10 μM 2,5-dimethyl-*p*-benzoquinone (E_{m7} = +180 mV), 20 μM *o*-naphthoquinone (E_{m7} = +145 mV), 2.5 μM N-

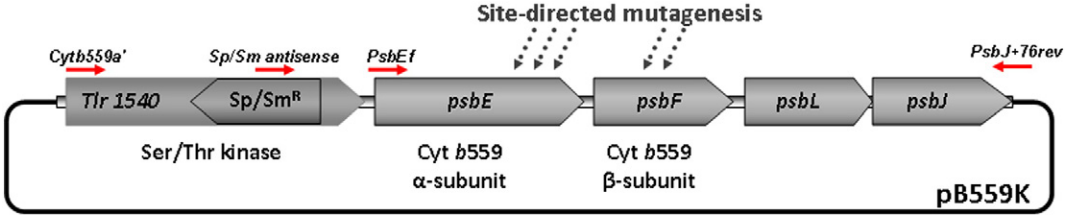

Fig. 1. Scheme of the plasmid pB559K used for the construction of site-directed mutants of cytochrome *b*559. Red arrows point out the positions of the primers used for the sub-cloning of the chromosomic region of *T. elongatus* containing the psbEFLJ operon plus the 3′ end of the trl1540 gene, and the primers for mutant screening and segregation. An antibiotic resistance cassette was introduced anti-sense inside the tlr1540. For more information see the Material and methods section.

methylphenazonium methosulfate (E_{m7} = +80 mV), 10 μM N-methylphenazonium ethosulfate (E_{m7} = +55 mV), 20 μM duroquinone (E_{m7} = +10 mV) and 30 μM 2-methyl-*p*-naphthoquinone (E_{m7} = 0 mV). Experiments were done at 20 °C under an argon atmosphere and continuous stirring.

Reductive titrations were performed by first oxidizing the samples to $E_h \approx +450$ mV with potassium ferricyanide and then reducing it stepwise with sodium dithionite. For oxidative titrations, the samples were first reduced to $E_h \approx +100$ mV with sodium dithionite and then they were oxidized stepwise with potassium ferricyanide. In both cases, after the addition of potassium ferricyanide or sodium dithionite, the absorption spectrum between 500 and 600 nm and the redox potential of the solution were simultaneously recorded using, respectively, an SLM Aminco DW2000 UV–vis spectrophotometer (USA) and a Metrohm Herisau potentiometer (Switzerland) provided with a combined Pt-Ag/AgCl microelectrode (Microelectrodes Inc., USA). Differential spectra of Cyt *b*559 in PSII core complexes were obtained by subtracting the absolute spectra recorded at each solution redox potential during titrations from the spectra of the fully oxidized state of the cytochrome (reductive titrations) or from the spectra of the fully reduced state of the cytochrome (oxidative titrations). The absorbance differences at 559–570 nm for Cyt *b*559 obtained from these spectra were normally converted into percentages of reduced cytochrome and plotted versus E_h. The E_m values were then determined by fitting the plots to the Nernst equation for a one-electron carrier ($n = 1$) with 2 components, and using a non-linear fitting option in Origin 7.5 (Microcal Software).

2.7. Thermoluminescence measurements

Thermoluminescence (TL) glow curves of *T. elongatus* cell suspensions were measured using two similar home-built apparatuses designed by Dr. Ducruet (Saclay, France) for standard (TL; 0–85 °C) and high temperature measurements (HTL; 10–160 °C). A detailed description of these systems can be obtained elsewhere [41–45]. Briefly, temperature regulation, signal recording and flash sequences were driven by a computer through a National Instrument DAQ-Pad1200 interface, using dedicated software. Temperature regulation was performed by means of a Marlow thermoelectric "Peltier" element powered by a variable (0 to 5 A) computer-driven power supply. Luminescence emission was detected by a H5701-50 Hamamatsu photomultiplier module. Illumination was performed through a light guide parallel to the photomultiplier, both of them being attached to the same stand sliding horizontally from the illumination to the measuring position. Single turn-over flashes were provided by a xenon white light (Walz XST-103). TL signals were analyzed with dedicated programs described in Ducruet [42].

For TL measurements, cell suspensions from *T. elongatus* cultures were collected by centrifugation and suspended in 40 mM MES pH 6.5, 15 mM $MgCl_2$, and 15 mM $CaCl_2$ at 100 μg Chl ml^{-1}. Then, they were frozen at −80 °C for half an hour. After slow thawing, the cell suspension was incubated on ice in darkness. Typically, 200 μl of cell suspensions were incubated in the darkness for 3 min at 45 °C, then cooled to 1 °C for 1 min and illuminated at the end of this period with different numbers of saturating single turn-over flashes (separated by 1 s) of white light through an optic fiber. Luminescence emission was then recorded while warming samples from 0 °C to 85 °C at a heating rate of 0.5 °C per s. For HTL measurements, cyanobacterial cell suspensions from *T. elongatus* cultures, equivalent to 7.5 μg Chl, were filtered through a cellulose ester membrane (0.22 μm, diameter). Then, the membrane with the dehydrated cell suspension was placed on the sample cuvette and pressed with a metal washer in order to ensure thermal contact with the Peltier plate. N_2 gas was flushed on the sample 15 min before and during experiments in order to desiccate samples and prevent any oxidation induced by high temperatures. Luminescence emission was then recorded while warming samples from 10 °C to 160 °C at a heating rate of 0.1 °C per s.

2.8. Oxidation–reduction kinetics measurements

The changes in the oxidation–reduction state of Cyt *b*559 induced by selective illumination of PSII were measured by using an SLM Aminco DW2000 UV–vis spectrophotometer in its dual wavelength mode. The absorbance changes at 559–570 nm were measured at 20 °C in a 3-ml cuvette containing the PSII particle suspension (50 μg Chl ml^{-1}) in different buffers. Illumination with an actinic light of PSII was performed by using a halogen lamp whose light was filtered by a narrow-band filter (Baird Atomic) with a band-width of 10 nm and maximal transmittance at 650 nm (70 W m^{-2}). An extra filter with maximal transmittance at 565 nm with a band-width of 50 nm (Oriel 7240) was inserted between the spectrophotometer photomultiplier and the sample compartment to allow the passage of reference and measurement lights and to prevent the passage of the actinic light.

3. Results

The aim of this work was to study the physiological role of the Cyt *b*559 (most precisely of its HP form) by changing its redox potential and/or the ratio between the HP and IP forms. Based in the 3-D structure of the Cyt *b*559 [4,6,7,36], in the conservation of different amino acids of the known sequences and in theoretical studies about the factors influencing the redox potential [46,47], a series of twelve amino acids around the heme were selected to be mutated in the thermophilic cyanobacterium *T. elongatus*. Viable cells were obtained from nineteen of the twenty-one mutants scheduled (Supplementary Table II). In this work we have analyzed in depth six of the mutant strains constructed: five in the α-subunit (I14A, I14S, R18S, I27A and I27T) and one in the β-subunit (F32Y) (Fig. 2).

3.1. Construction of site-directed mutants of cytochrome b559

To generate mutants of *T. elongatus* containing a modified Cyt *b*559, the genome region containing the genes coding for the α and β-subunits of Cyt *b*559 (*psbE* and *psbF* respectively), and the PsbL (*psbL*) and PsbJ (*psbJ*) proteins (forming an operon) (Fig. 1) was amplified by PCR and cloned. The amplified region also included as part of the *tlr1540* gene encoding a serine–threonine kinase. A plasmid was constructed in which the *tlr1540* gene was interrupted by insertion of a Sp/Sm resistance cassette (Fig. 1). The site-directed mutations in *psbE* and *psbF* genes were introduced in the plasmid in which the *tlr1540* gene had been previously interrupted. Since the absorbance spectra of the Cyt *b*559 and Cyt b_6f complex are similar, the measurement of the E_m of Cyt *b*559 cannot be done using whole cells or thylakoids. In order to do these measurements, very active PSII complexes must be isolated. For this reason, the WT' mutant strain of *T. elongatus*, which contains a His-tagged CP43, was used as a receptive strain of plasmids containing the mutated *psbE* and *psbF* genes. It was already demonstrated that this strain allows the isolation of very active and entire PSII complexes [37]. The plasmids were introduced into WT' cells by electroporation. The interrupted *tlr1540* and point-mutated *psbE* and *psbF* genes were incorporated into the cyanobacterium genome by homologous double recombination. A plasmid containing the *psbE* and *psbF* genes (without mutations) and the *tlr1540* gene interrupted by the Sp/Sm resistance cassette was introduced into WT' cells in order to create the control strain WT''. This strain lacks the serine–threonine kinase protein encoded by the *tlr1540* gene, but presents a phenotype similar to the WT, respecting PSII activity. For details of the construction of mutants see the Material and methods section. From the twenty-one plasmids constructed nineteen viable mutants were obtained (Supplementary Table II). The mutations αG34V and βF32S were lethal. Most probably these mutations induced an important modification of the interaction between α and β-subunits, leading to the loss of the heme.

In this work, six of the mutant strains obtained have been characterized. Four of them contain modifications in apolar residues affecting the

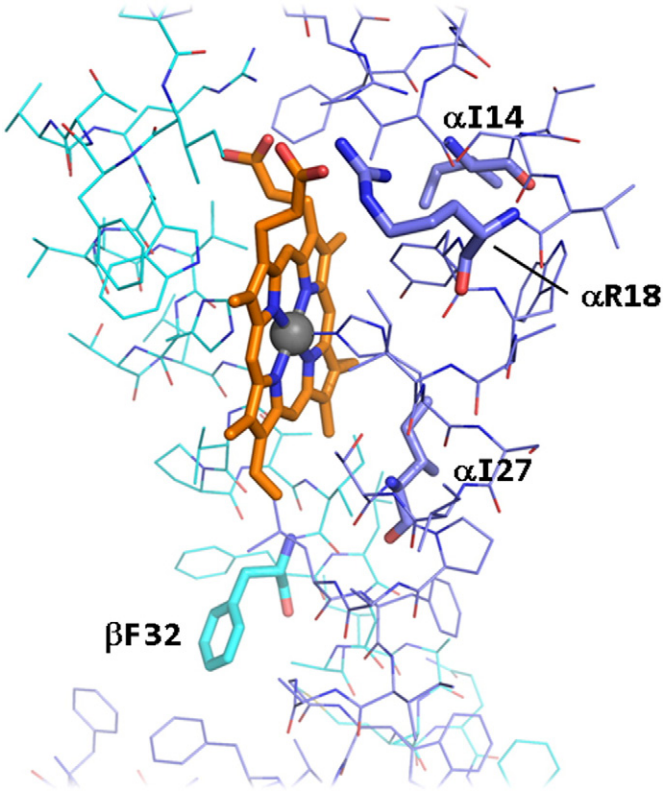

Fig. 2. Three dimensional structure of the heme pocket of cytochrome *b*559. The conserved residues of cytochrome *b*559 selected for site-directed mutagenesis are shown (Ile14, Arg18, Ile27 in the α-subunit, and Phe32 in the β-subunit). The heme group is represented as orange sticks. Figures have been made using PyMol and the PDB file 3ARC.

hydrophobicity of the environment of heme: αI14A, αI14S, αI27A and αI27T. In another, the arginine forming an ionic bond with the heme propionate was changed by a serine (αR18S). In the last mutant, Phe32 in the β-subunit was replaced by a tyrosine. This mutation could affect the relative position between α and β-subunits affecting the binding of the heme to the histidines [22,23].

3.2. Effect of mutations on the redox properties of cytochrome b559

As described in the Material and methods section, almost 100% of the total Cyt *b*559 was initially reduced in oxygen-evolving dark-adapted PSII core complexes of WT and all the mutant strains (see Supplementary Fig. 1).

The first step in the phenotypic characterization of the mutant strains was the determination of the E_m of Cyt *b*559. This parameter is one of the most important biophysical characteristics of a cytochrome because it usually determines the biological function of the protein. Potentiometric titrations at pH 6.5 of Cyt *b*559 in PSII core complexes from WT" (Fig. 3) and the six mutated strains of *T. elongatus* studied (Fig. 4) have been carried out in order to determine the number of redox potential forms, the ratio between them and their E_m values. Redox titrations in both oxidative and reductive sequences with identical results have been obtained. This increased confidence that titrations have been successfully performed at equilibrium.

Fig. 3 shows a representative reductive and oxidative potentiometric titration of PSII core complexes from the WT" control strain of *T. elongatus* at pH 6.5. Differential spectra in the α-band region of Cyt *b*559 have been obtained by subtracting the spectrum obtained at a potential of +480 mV, at which the Cyt *b*559 is completely oxidized from those recorded during the course of the redox titration (insets of Fig. 3). A plot of the percentages of reduced Cyt *b*559, obtained from these difference spectra, versus E_h could be fitted to a Nernst equation in accordance with a one-electron process ($n = 1$) for two redox components (Fig. 3). It clearly indicated the existence of two different Cyt *b*559 components with E_m values of +395 mV (accounting for approximately 85% of the total amount of protein) corresponding to the HP form and +248 mV (approximately 15% of the total amount of protein) corresponding to the IP form. No low potential (LP) form of Cyt *b*559 was present in these PSII preparations. Table 1 shows the average values (mean) of six independent experiments for the E_m and percentages of the two HP and IP forms of Cyt *b*559. These values were similar to those already published by our research group [48]. An identical result was obtained from the oxidative potentiometric titration (Fig. 3).

Representative potentiometric reductive titrations of Cyt *b*559 in the six mutated strains of *T. elongatus* studied in this work are shown in Fig. 4. The proportion of the HP and IP forms of Cyt *b*559 and the E_m values were obtained as described in Fig. 3. The average values of E_m and percentages of the HP and IP forms are also shown in Table 1. All the mutations induced a slight decrease (15–35%) of the percentage of the HP form of Cyt *b*559 (Fig. 4 and Table 1). In addition, the E_m values of the HP and IP forms were also lower than in the WT" strain. The most affected mutated Cyt *b*559 were αR18S and αI27T strains with E_m values of the HP form of +330 and +308 mV, respectively (Table 1).

3.3. Effect of mutations on cell growth and PSII activity

The photosynthetic growth rates of WT" and the six Cyt *b*559 mutant strains were similar during the first three days of growth at 45 °C and at 100 μE m^{-2} s^{-1} of light intensity (Fig. 5A). Then, a slight but significant decrease of the growth rate of the αR18S mutant strain was observed (see also the section: 'Effect of the αR18S mutation on light sensitivity'). However, all the other mutants grew at a similar rate than the WT". Under a lower light intensity (40 μE m^{-2} s^{-1}), all the mutant cells, including αR18S, grew at the same rate than the WT" during more than one week (data not shown).

Mutations in the Cyt *b*559 did not significantly affect the oxygen evolving activity of PSII in whole cells (Table 1). Control (WT") and mutated strains had similar oxygen evolving activities (230–250 μmol

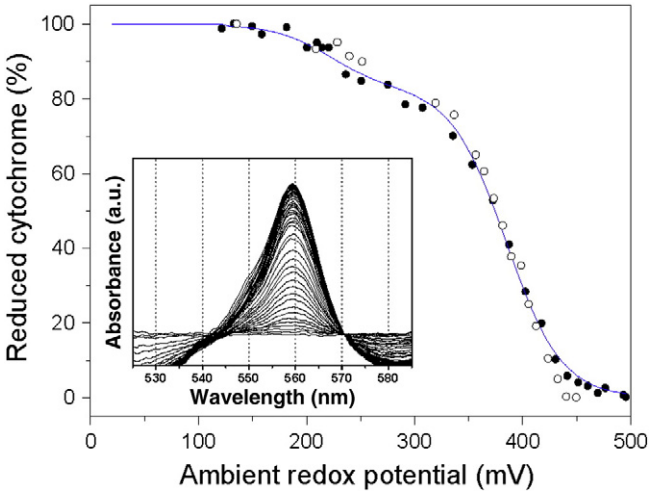

Fig. 3. Potentiometric redox titration of cytochrome *b*559 in isolated PSII complexes from the WT" strain of *T. elongatus*. The figure represents the plot of the percentages of reduced cytochrome *b*559 obtained from the absorbance differences at 559–570 nm versus ambient redox potentials. These data were obtained from the difference absorption spectra described below. Closed and open circles represent the data obtained in a reductive and an oxidative titration, respectively. The solid blue curve is the best fit of the experimental data to the Nernst equation in accordance with one-electron processes ($n = 1$) for two components with E_m of +248 mV (15%) and +395 mV (85%). The inserted graph shows the difference absorption spectra in the α-band region of cytochrome *b*559 obtained by subtracting absolute spectra recorded during the course of the redox titration minus the spectrum recorded at +450 mV. For simplification, only spectra from the reductive titration are included in the figure. For other details see the Material and methods section.

O_2 mg Chl^{-1} h^{-1}). However, all mutations slightly decreased the oxygen evolution activity in the isolated PSII core complexes (Table 1). Highly active PSII complexes (3240 μmol O_2 mg Chl^{-1} h^{-1}) were isolated from control cells. PSII complexes isolated from the Cyt *b*559 mutated strains presented an activity of about 25% lower than that of the WT" PSII.

The effect of mutations on the TL emission bands of PSII was also studied. The TL emitted at physiological temperatures arises from charge recombination from S_2 with Q_A^- (the Q band) and from $S_{2/3}$ with Q_B^- (the B band) (for review [49–51]). The relative stability of these charge pairs is reflected in the luminescence emission

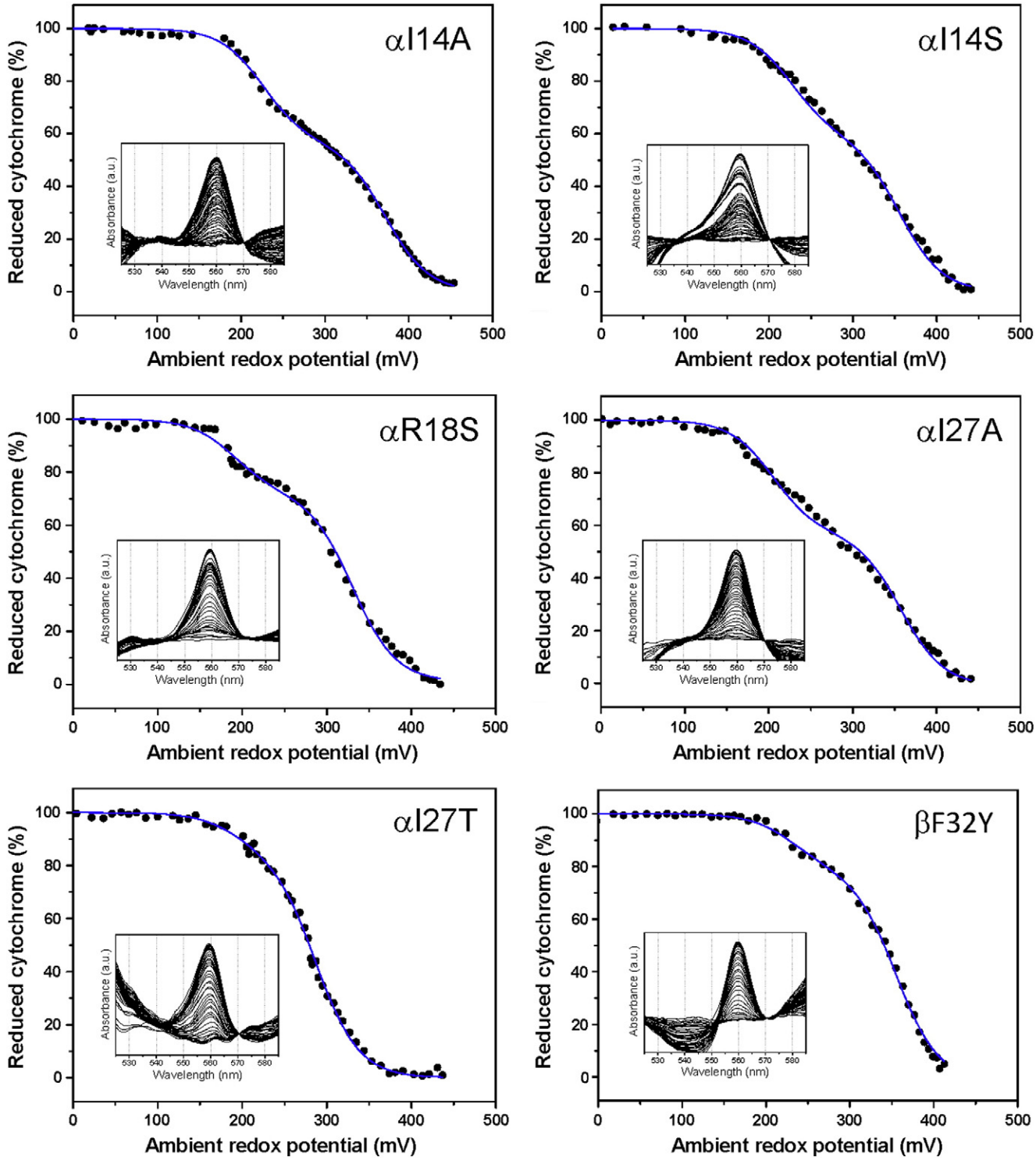

Fig. 4. Effect of mutations on the redox properties of cytochrome *b*559. Figures represents the plot of the percentages of reduced cytochrome *b*559 obtained from the absorbance differences at 559–570 nm versus ambient redox potentials during the course of the reductive potentiometric titrations of cytochrome *b*559 in isolated PSII complexes from cytochrome *b*559 mutant strains. The inserted graphs show the difference absorption spectra in the α-band region of cytochrome *b*559 obtained by subtracting absolute spectra recorded during the course of the redox titration minus the spectrum recorded at about +450 mV. The solid blue curves are the best fits of the experimental data to the Nernst equation in accordance with one-electron processes ($n = 1$) for two components with different E_m values. The E_m values (average values of six independent experiments) obtained are shown in Table 1. For other details see the Material and methods section.

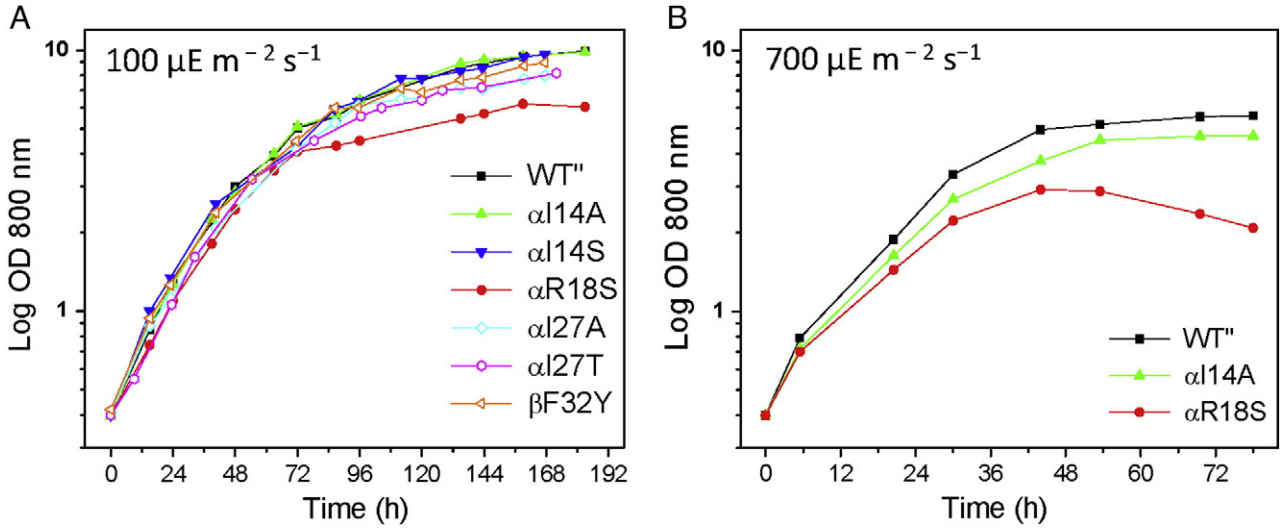

Fig. 5. Growth curves of WT" and cytochrome *b*559 mutant strains. *T. elongatus* cells were grown in "bottles" (out of incubators) immersed in a water bath at 45 °C and in DTN-medium agitated by bubbling of a CO_2-enriched atmosphere (1%). The cultures were illuminated continuously with a white light of 100 (A) or 700 µE m^{-2} s^{-1} (B) light intensity. For further details see the Material and methods section.

temperature with the Q band occurring at a lower temperature than the B band [49]. These charge recombination reactions are influenced by the redox potential of quinones Q_A and Q_B and S states of the oxygen evolving complex, and by the stability of the reduced quinones and oxidized S states. Due to the interactions between the Cyt *b*559 and D1 protein, it is possible that mutations in Cyt *b*559 may induce changes in the E_m or stability of Q_B, which is reflected in changes on the TL B band.

The TL pattern of unfrozen cells is complicated and variable due to different values of the dark-stable transmembrane proton (and/or electrochemical) gradient that changed from one culture batch to another. In this work, the TL experiments were performed using frozen and thawed cells where the pattern of TL was stable and independent of cell batch [39,52].

Fig. 6A compares the B band of TL obtained after one flash (corresponding to $S_2Q_B^-$ recombination) in cells from WT" and Cyt *b*559 mutant strains. The maximum temperature of the B band obtained after one flash was similar (about 61 °C) in WT" and αI14A, αI27T and βF32Y mutant cells. Mutants αI14S, αR18S and αI27A presented a slight shift (2 °C) to higher temperatures. Additionally, the intensities of the B bands were slightly lower in most of the mutated strains. The most important decrease of the intensity was observed in αI14S (30%) and αR18S (20%) strains.

The intensity of the B band exhibited a typical four-oscillation period with maxima after the 2nd and 6th flashes in WT" and most mutated strains of *T. elongatus* (Fig. 6B). The amplitude of the oscillation was smaller in all the mutants than in WT". This pattern of intensity oscillation of the B band is due to the fact that in dark-adapted PSII the ratio S_0:S_1 is around 25:75 and Q_B:Q_B^- around 40:60 [51]. Thus, after one single flash, the S_1Q_B centers will go to the luminescence-emitting state $S_2Q_B^-$, generating a B band. Two flashes induced the greatest B band glow curve because they generate an important amount of PSII centers in both $S_2Q_B^-$ and $S_3Q_B^-$ luminescence states. Besides, the TL yield from the latter recombination is higher than that from the former by a factor of 1.7–2.0 [53]. Interestingly, in several measurements done with the mutant αR18S (about 66%), the maximum of the intensity oscillation was in the third flash instead of in the second flash (Fig. 6C), suggesting that the mutation has a small effect on the dark state of PSII: a higher reduction of the PQ pool and/or a higher concentration of S_0 in dark

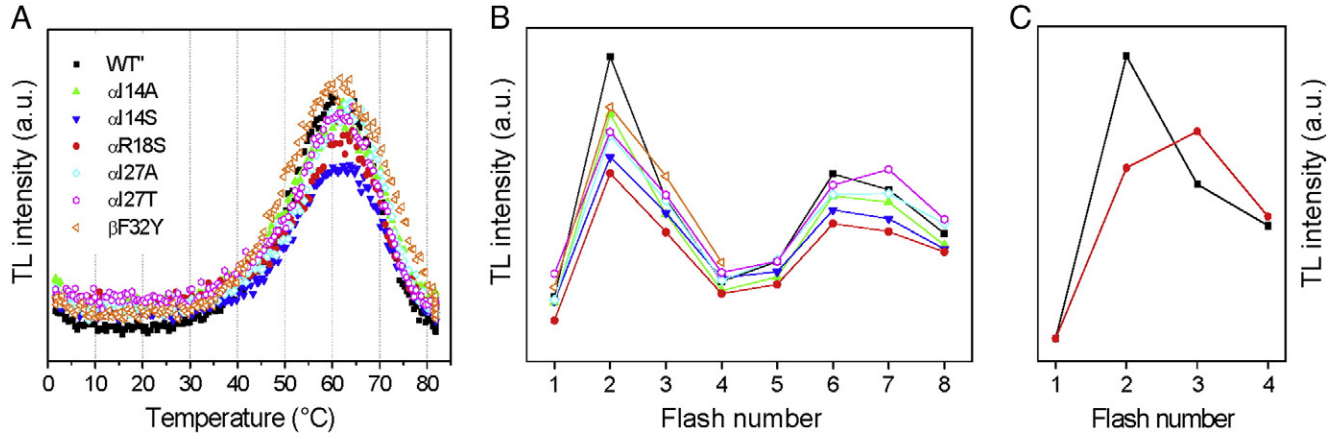

Fig. 6. Thermoluminescence emissions from WT" and cytochrome *b*559 mutants. (A) Thermoluminescence glow curves (B bands) of WT" and cytochrome *b*559 mutant cells of *T. elongatus* recorded after one flash. (B) Oscillation of the intensity of B band of WT" and cytochrome *b*559 mutant cells as a function of flash number. Cultures were collected by centrifugation and suspended on 15 mM $MgCl_2$, 15 mM $CaCl_2$ and 40 mM MES pH 6.5 buffer, at 100 µg Chl ml^{-1}. Then, they were frozen at −80 °C and thawed in darkness. Typically, 200 µl of cell suspensions were incubated in the darkness for 3 min at 45 °C, then cooled to 1 °C for 1 min and illuminated at the end of this period with different numbers of flashes (separated by 1 s) of white light. Luminescence emission was then recorded while warming samples from 0 °C to 85 °C at a heating rate of 0.5 °C per s. Intensities (B) were obtained from the component analysis of the curves of thermoluminescence, as described in the Material and methods section. In about 66% of the experiments performed (C) the mutant αR18S showed a different pattern of oscillation of the intensity of B band with a maximum in the third flash. For further details see the Material and methods section.

adapted cells. This heterogeneity may be related to the higher sensitivity to light observed in the αR18S Cyt *b*559 mutant strain that will be discussed later.

3.4. Effect of the αR18S mutation on light sensitivity

The αR18S mutant strain showed a significantly slower growth rate compared to those of WT" and the other mutant strains (data shown only for I14A strain, as example) when cells were grown under rather high light conditions (700 μE m^{-2} s^{-1}) (Fig. 5B). After 48 h of growth the cells began to die and the cellular concentration in the culture progressively decreased. These results suggested that the αR18S mutant is much more sensitive to high light conditions than the WT" and the other mutant strains.

The light sensitivity of the αR18S mutant was further studied by following the decrease of oxygen evolution activity during exposure of WT" and mutant cells to high light intensities (1500 μE m^{-2} s^{-1}) (Fig. 7). The measurements were done in the presence of lincomycine, an inhibitor of protein synthesis to avoid photoinhibition recovery by replacement of the damaged D1 protein. Most of the Cyt *b*559 mutants presented a higher sensitivity to high irradiance than WT" cells, the most affected being the αR18S strain. The decrease of the oxygen evolution activity was significantly faster in this mutant confirming its higher sensitivity to photoinhibitory conditions.

In photosynthetic cells, photoinhibitory conditions (as exposure to high light intensities) increase the probability to generate very reactive and toxic oxygen species in PSII. These species could initiate the peroxidation of unsaturated lipids in membranes. The level of lipid peroxidation in photosynthetic membranes can be measured by the HTL technique [54]. Several luminescence high temperature bands (HTL bands) have been observed without prior illumination at temperatures above 60 °C [54]. A broad HTL band centered near 130 °C (known as the HTL2 band) is generated because of the thermal radiative decomposition of lipid peroxides that, in turn, leads to the formation of carbonyl groups in a triplet state followed by migration of excitation energy toward chlorophylls [54]. It has been demonstrated that this band is indicative of oxidative damage in stressed plants [54,55]. The amplitude of this band has been well correlated with the accumulation of malondialdehyde, an indicator of lipid peroxidation in standard chemical tests [54].

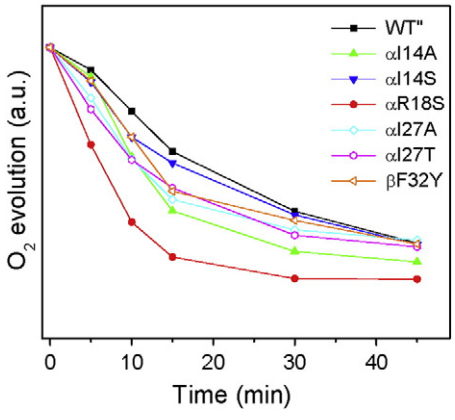

Fig. 7. The effect of high intensity illumination on oxygen evolution activity of PSII in WT" and cytochrome *b*559 mutants. *T. elongatus* cells from liquid cultures in a stationary growth phase were precipitated and suspended in 40 mM Mes pH 6.5, 15 mM $MgCl_2$, 15 mM $CaCl_2$, and 25% (v/v) glycerol at a concentration of 10 μg Chl ml^{-1} in the presence of 100 μg ml^{-1} of lincomycin and 1 mM DCBQ, as an electron acceptor. Samples were incubated at 45 °C and exposed to high intensity white light (1500 μE m^{-2} s^{-1}) during different time periods. After the treatment, oxygen evolution was measured at 25 °C by polarography using a Clark-type oxygen electrode (Hansatech) as described in the Material and methods section. Data are means of three independent experiments. The initial activity of oxygen evolution at $t = 0$ for all strains is normalized to 1. The initial values of oxygen evolution of each strain are given in Table 1.

We applied the HTL technique to detect lipid peroxidation in *T. elongatus* cells. There are no many studies in which this technique has been applied to investigate lipid peroxidation in cyanobacteria [56]. Fig. 8 shows that a clear HTL2 band with the maximum at 140 °C was present in αR18S mutant cells. This band was almost not detectable in WT" cells. These measurements have been done by using cells from four day growth cultures at 45 °C and under standard light intensity conditions (100 μE m^{-2} s^{-1}) (Fig. 5A). Thus, the higher sensitivity of the αR18S Cyt *b*559 mutant to light was also observed in cells grown under medium light intensities. The band peaking at about 61 °C can be a HTL1 band due to mixtures of aldehydes and hydrogen peroxide that excites chlorophyll through a dark induced carbonyl triplet [57] or a CL-named band originating from the thermally stimulated production of an active oxygen species that results in lipid peroxidation [58]. This band was also very small in WT" cells.

3.5. Cytochrome b559 photoreactions in inactive PSII complexes

A deficient plastoquinone oxidase activity of the Cyt *b*559 in the αR18S mutant strain could be the reason for its higher sensitivity to strong irradiance and the possible higher reduction of its plastoquinone pool. To clarify this proposal, we have studied the photooxidation and re-reduction reactions of the Cyt *b*559 under conditions in which the water oxidation system in PSII is not working. It is well known that the Cyt *b*559 can give electrons to $P680^+$ via a carotenoid molecule under conditions in which the oxygen evolving complex is inactivated or slowed down (for example, at basic pH) [59]. It is important to state that the relative proportion between the two redox potential forms of Cyt *b*559 was not significantly altered by pH, between pH 6.0 and 8.5, in PSII core complexes of *T. elongatus* in WT" and all of the mutant strains studied (data not shown; see also ref. [11]). In the darkness, the photooxidized Cyt *b*559 can then be reduced by electrons from Q_B^- or by the pool of reduced plastoquinone (PQH_2) [60]. This secondary electron transport chain was proposed to be photoprotective [18,59,60]. The changes in the oxidation and reduction state of Cyt *b*559 can be followed by simultaneous measurements of the changes in the absorption at 559 nm (the maximum of the Cyt *b*559 α-band) minus 570 nm (an isosbestic point). The absorbance difference between these measurements gives the changes of the redox state of the Cyt *b*559.

The study was focused in this work on comparing the reactions in the WT" and the αR18S mutant strains. Fig. 9 shows the light-induced absorbance changes of Cyt *b*559 in *T. elongatus* PSII complexes from WT" and αR18S strains, under conditions that prevent electron transport in the PSII donor side (at basic pH). Illumination with a 650 nm

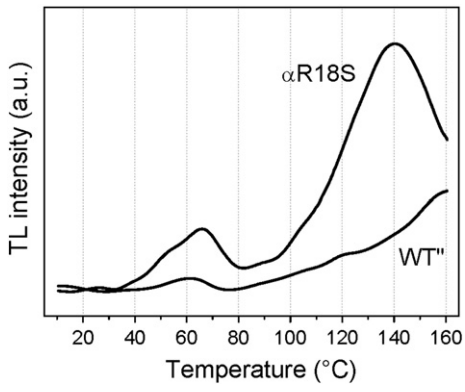

Fig. 8. High temperature thermoluminescence glow curves of the WT" and αR18S mutants. *T. elongatus* cell suspensions from four day *T. elongatus* growth cultures, equivalent to 7.5 μg Chl, were filtered through a cellulose ester membrane (0.22 μm, diameter) and placed on the sample cuvette. After a dark adaptation period of 1 min at 10 °C, luminescence emission was recorded while warming samples from 10 °C to 160 °C at a heating rate of 0.1 °C per s. For further details see the Material and methods section.

red light absorbed by PSII induced very small changes in the absorbance at 559 nm (relative to 570 nm) in control PSII complexes suspended in the optimum medium for donor side activity (40 mM Mes pH 6.5, 15 mM $MgCl_2$, 15 mM $CaCl_2$, 25% (v/v) glycerol). However, red light irradiation of PSII complexes suspended in 50 mM Tricine–KOH (pH 8.0), in which the water oxidation system is impaired (the rate of oxygen evolution being ten times lower than before; data not shown), induced a large biphasic photooxidation of the reduced Cyt *b*559 in WT" and the mutant (Fig. 9). After the red light illumination was turned off, absorbance at 559–570 nm increased indicating the reduction of the previous oxidized fraction of Cyt *b*559. The spectra of the two phases of oxidation and the reduction indicate that these light-induced absorbance changes correspond mostly to the cytochrome *b*559 (Supplementary Fig. 2). Whereas in WT" PSII complexes this reduction was very important (about 80% of the previous oxidized fraction of Cyt *b*559 after 5 min; Fig. 9), for the αR18S mutant the fraction of Cyt *b*559 reduced in the darkness was significantly smaller (about 40% after 5 min; Fig. 9). Another important difference in the reduction of Cyt *b*559 in the darkness between WT" and the mutant strain was also observed: whereas in WT" the rate of the reaction (half-time) was 15 s, in the αR18S mutant the reaction was significantly slower (about 40 s). Therefore, these experiments have revealed a significant alteration in the αR18S mutant on the kinetics and yield of the reduction of Cyt *b*559 in darkness by electrons from Q_B^- or the PQH_2 pool.

4. Discussion

The main objective of this work was to study the role of the HP form of Cyt *b*559. For this, strains of the thermophilic cyanobacterium *T. elongatus* with mutations in Cyt *b*559 which could induce changes in its redox potential were constructed. Phenotypic characterization of some of these mutants has led to progress in understanding the possible role of this cytochrome within PSII.

Twenty one different variations in twelve amino acids (seven of the α-subunit and five of the β-subunit) with theoretical importance for the establishment of the special properties of the HP form of Cyt *b*559 and for its structural stability were selected (see Supplementary Table II). Viable cells were obtained from nineteen of the twenty one mutants scheduled. Positive colonies were not obtained for βF32S and αG34V strains probably because these mutations are lethal by affecting the interaction between the two subunits and, as a consequence the heme binding and hence the Cyt *b*559 stability. The βF32S mutant is comparable to the βF26S mutant described in the tobacco plant [61]. This mutation caused a severe phenotype in tobacco, but it was not lethal: PSII was significantly destabilized and its activity was very low. In addition, the plastoquinone pool was largely reduced [22,23]. The fact that the mutation causes important changes in PSII activity could explain why we were unable to obtain the βF32S mutant. αGly34 is a critical residue in the interaction between the two subunits, possibly forming hydrogen bonds which stabilize the helix–helix interaction [62]. This mutation might disrupt the interaction between helixes and therefore the assembly of Cyt *b*559 and the PSII complex.

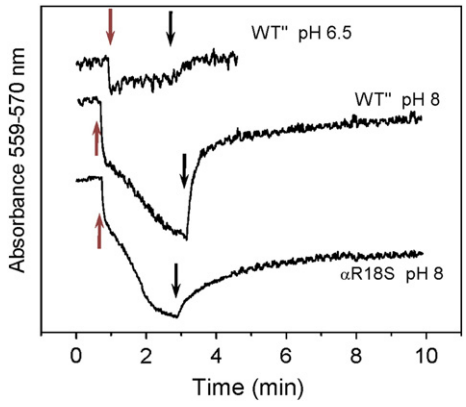

Fig. 9. Photoreactions of cytochrome *b*559 in PSII core complexes from WT" and αR18S mutants. Cyt *b*559 redox changes were measured by the changes in absorbance at 559–570 nm induced by illumination with a red light at 650 nm (red arrow) and subsequent removal of the lighting (black arrow) by dual wavelength spectroscopy as described in the Material and methods section. The first trace shows the photoreactions measured in the WT" strain in 40 mM Mes pH 6.5, 15 mM $MgCl_2$, 15 mM $CaCl_2$, and 25% (v/v) glycerol. The second and third traces correspond to the absorbance changes measured in PSII complexes from WT" and αR18S strains in 50 mM Tricine–KOH pH 8.0, respectively. At pH 8.0 the water oxidation system is almost impaired and the relative proportion between the two redox potential forms of cytochrome *b*559 was not significantly altered in WT and R18S strains.

4.1. The redox properties of cytochrome b559

Six of the nineteen mutants of Cyt *b*559 obtained have been characterized in detail in this work. Mutations that could affect the hydrophobicity of heme niche (αI14A, αI14S, αI27A, αI27T), the interaction between the two subunits (βF32Y) and the ionic bond between a residue of the protein and the heme propionate (αR18S) were selected.

None of the six mutant strains of *T. elongatus* studied in this work were significantly affected in their patterns of cell growth in standard conditions (Fig. 5A). Similar oxygen evolving activities were observed in cells of all strains (Table 1). In contrast, in PSII preparations of all mutated strains a significant decrease of PSII activity was observed. This reduction in PSII activity could be due to instability in the structure of PSII induced by mutations of Cyt *b*559. It does not appear to be related to the alteration of the E_m of the HP form of Cyt *b*559 because mutants in which the E_m was changed more (αR18S and αI27T) showed declines in activity similar to those of other mutant strains.

Redox potentiometry experiments conducted in this work showed no significant differences in the absorption spectra of the mutated Cyt *b*559 compared to that of the WT" strain. This indicated that the studied mutations does not substantially affect heme coordination or cytochrome overall structure. In contrast, PSII preparations from all mutants presented a significantly lower percentage of the HP form of Cyt *b*559 than the WT" (Table 1). As already said, the proportion of PSII centers with the HP form of Cyt *b*559 depends on the integrity of the complex [3,8,10,63,64]. Many authors have proposed that the presence of a hydrophobic environment around the heme group is a key factor for the stability of the HP form [8,10,11,65–67]. The conversion of the HP to the IP form can be a consequence of the breakage of a hydrogen bond between one of the histidines coordinating the heme and the protein [8,10]. This would cause the opening of the heme niche to the aqueous environment stabilizing the ferric state and lowering, consequently, the E_m. In the Cyt *b*559 mutants characterized in this work the conversion of HP form into IP could be a consequence of structural changes in the cytochrome preventing the maintenance of the hydrogen bond necessary for the stabilization of the HP form. Our results seem to indicate that the aliphatic amino acids of the α-subunit Ile14 and Ile27 are very important residues to the maintenance of the structural or/and hydrophobic conditions needed for the preservation of the HP state of the cytochrome.

The mutations of amino acid residues in the heme environment of Cyt *b*559 investigated in this work not only led to the partial conversion of HP into the IP form but also induced the change of the E_m values of both forms (Table 1). While a slight decrease on the E_m between 25 and 40 mV was measured in αI14A, αI14S, αI27A and βF32Y mutants, a more important decline was observed in αR18S (64 mV) and αI27T (86 mV). A similar decrease of 30 mV compared to WT" was observed in the IP form of all studied mutants, except in βF32Y. Taking into account that the aliphatic residues Ile14 and Ile27 of the α-subunit are at around 4 Å of heme (Fig. 2), it is probable that a hydrophobic interaction between the heme and such residues exists. This hydrophobic interaction could be therefore a key factor in establishing the extremely

positive E_m of the HP form [68]. Substitution of the isoleucine by a smaller (alanine in αI14A and αI27A) or polar (serine in αI14S) residue would alter this interaction. The decrease of 86 mV in the E_m of the HP form in the mutant αI27T compared to WT" may indicate that the apolar environment determined by Ile27 and/or the hydrophobic interaction with the heme also substantially contributes to the establishment of the high redox potential of the HP form. On the other hand, several authors have suggested that the electric field created by the positive charges of the arginines near the heme affects the E_m of the Cyt *b*559 [46,69]. The disappearance of the positive charge of the arginine being replaced by serine in the mutant αR18S could explain the decrease in 64 mV in the E_m of the HP form observed in this mutant. The positive charges near the propionate group may favor the stabilization of the reduced form of heme, thereby maintaining its high redox potential (Fig. 2).

4.2. Sensitivity to high irradiance in the mutant αR18S

The largest phenotypic differences compared to WT" have been shown by the mutant αR18S. Cells of this mutant showed a significant decrease in the growth rate after 72 h of culture when grown at 100 μE m^{-2} s^{-1}. Under photoinhibitory conditions (700 μE m^{-2} s^{-1}), the αR18S strain showed a retarded growth relative to the WT" strain and after 48 h the level of cell proliferation was decreasing progressively (Fig. 5B). These results strongly suggested that the αR18S mutant strain is more sensitive to high irradiance than the WT" strain. The experiments of the effect of phototoinhibitory illumination in the oxygen evolution (Fig. 7) confirmed the increased sensitivity of PSII to high irradiance in the αR18S strain. Other mutants such as the αI14A and αI27T strains also showed a higher sensibility to high light in comparison with WT" but lower than that of αR18S. These results agree with the observations described for various arginine mutants in the α-subunit of Cyt *b*559 (R18E and R18G) in *C. reinhardtii* [70] and in both α and β-subunits (αR7E, αR17A and βR17L) in *Synechocystis* sp. PCC 6803 [14].

Thermoluminescence measurements (Fig. 6C) suggested that the dark concentrations of S_0 and/or reduced plastoquinone can be higher in the αR18S mutant strain. A more reduced plastoquinone pool was also observed in the R17Lβ *Synechocystis* sp. PCC 6803 mutant [14]. A high concentration of Q_B^- in the PSII caused by a reduced plastoquinone pool may increase the probability to generate the very reactive and toxic specie $^1O_2$ (singlet oxygen), that could initiate the peroxidation of unsaturated lipids in photosynthetic membranes. Recently, new lines of evidence have been provided that the superoxide anion radical formed on the PSII acceptor side results in the formation of carbon-centered radicals that may also initiate lipid peroxidation [71]. Indeed, a high level of lipid peroxidation has been observed in high temperature thermoluminescence experiments (HTL) (Fig. 8) of αR18S mutant cells grown with standard (no photoinhibitory) culture conditions. A modified interaction between Cyt *b*559 and Q_B or the plastoquinone pool proposed for the tobacco F26Sβ Cyt *b*559 mutant [22] could explain this higher sensitivity to high irradiance of the αR18S mutant.

Kinetics measurements of light induced oxidation and dark rereduction of the Cyt *b*559 in the αR18S mutant (Fig. 9) confirmed this modification. It is important to note that Cyt *b*559 is mostly in its reduced state in dark adapted PSII core complexes. Our results showed that under conditions of a non-functional water oxidation system, once the Cyt *b*559 is oxidized by $P680^+$ after charge separation induced by a red light, the reduction of Cyt *b*559 by Q_B or the plastoquinone pool is largely modified in the αR18S mutant. Only 40% of the previously photooxidized Cyt *b*559 in the mutant was reduced in darkness in comparison with the 90% in the WT" strain. In addition, the rate of the reaction was significantly slower in the mutant compared to the WT" (40 s and 15 s of half-time, respectively). This suggested that the lowering of the E_m of the HP form in the mutant induced a significant alteration in the electron transfer from the acceptor site of PSII to Cyt *b*559. A significantly reduced difference in redox potential (ΔE_m) between the donor (Q_B^- or plastoquinone) and acceptor (Cyt *b*559) of electrons could explain the substantial decrease in the reaction rate observed in the mutant. This lower ΔE_m affects the difference of the free energy of the reaction (ΔG_0) and therefore its kinetic constant. Furthermore it also seems that there is a significant percentage of PSII centers in which the Cyt *b*559 remained oxidize indicating that in these centers there is no electron transfer reaction from Q_B or the plastoquinone pool to Cyt *b*559. A recent study has proposed that the arginines that establish ionic bonds with heme propionates could function as electron transfer pathways in the cytochromes [70]. The changes observed in the αR18S mutant in the reduction of Cyt *b*559 after its photooxidation may be caused not only by the change in E_m, but also by an alteration of the electron transfer from the acceptor side through the serine residue.

Several authors have proposed that the HP form of Cyt *b*559 would function as a redox reservoir participating in a cyclic electron transfer path to reduce to $P680^+$ when the water oxidation system does not work, thereby avoiding damage from this highly oxidizing form during photoinhibition [15,59]. Once oxidized, the very high E_m of the HP form may favor the Cyt *b*559 reduction by the plastoquinone pool via the Q_C site [12,22,23]. Thus Cyt *b*559 can be considered as a plastoquinol oxidase. Although the correlation between a higher sensitivity to high irradiance and a more reduced plastoquinone pool has already been observed in the tobacco F26Sβ and the R7Eα and R17Lβ Cyt *b*559 mutants of *Synechocystis* sp. PCC 6803, we are the first to measure the deficiency of the plastoquinol oxidase activity of the Cyt *b*559 mutants presenting a higher sensitivity to high irradiance. In the αR18S mutant the reduction of the HP form is significantly altered. Thus, during a photoinhibitory process the ability of Cyt *b*559 to reduce $P680^+$ would be gradually decreased, increasing the probability of damage induced by this extremely oxidizing cation $P680^+$ (E_m of 1.25 V; one of the most positive known in organic molecules [72]). In this mutant the partial blocking of the electron transfer from quinones increases the probability of the generation of very reactive and toxic species such as $^1O_2$ (singlet oxygen) and superoxide anion radical in PSII. In other mutants as αI14A and αI27A in which the maintenance of the HP form is also slightly altered, the ability of Cyt *b*559 to reduce $P680^+$ would also be decreased, increasing the probability of photoinhibitory damage.

5. Conclusions

The use of PSII preparations from *T. elongatus* of high integrity and activity allowed us to measure for the first time the influence of different Cyt *b*559 mutations on the E_m values of the HP form and on the reduction of Cyt *b*559 by the plastoquinone pool (or Q_B). Based on our results, we propose that the HP form of Cyt *b*559 may be the key element in the control of the secondary electron transfer reactions which protect PSII. An extremely positive redox potential would be necessary to ensure efficient Cyt *b*559 reduction by the PSII acceptor site and to function as an electron reservoir to reduce the oxidized β-carotene molecule and $P680^+$ replacing OEC function when it does not operate. The existence of three quinones, besides Q_A, in PSII core complexes of *T. elongatus* has been proposed [26,27]. The electron donor of Cyt *b*559 could be the new quinone Q_C. This proposal should be supported in the future with new experiments based on the use of mutants with modifications that significantly alter the Q_C site.

Supplementary data to this article can be found online at http://dx.doi.org/10.1016/j.bbabio.2014.02.024.

Acknowledgements

This work was supported by Grants BFU2007-68107-C02-01 and BIO2012-35271 from the Spanish Ministries of Science and Innovation and Economy and Competitiveness, respectively, and the PADI CVI-261 and BIO-022 from the Andalusia Government. All these Grants were partially financed by the EU FEDER Program. DK's work was

supported by CNRS and CEA. FG received a one year fellowship from CEA to work in DK's laboratory.

References

[1] B.A. Diner, G.T. Babcock, Structure, dynamics and energy conversion efficiency in photosystem II, in: D.R. Ort, C.F. Yocum (Eds.), Oxygenic Photosynthesis: The Light Reactions, Kluwer Academic Publishers, The Netherlands, 1996, pp. 213–247.

[2] J. Whitmarsh, H.B. Pakrasi, Form and function of cytochrome *b*-559, in: D.R. Ort, C.F. Yocum (Eds.), Oxygenic Photosynthesis: The Light Reactions, Kluwer Academic Publishers, The Netherlands, 1996, pp. 249–264.

[3] D.H. Stewart, G.W. Brudvig, Cytochrome *b*559 of photosystem II, Biochim. Biophys. Acta 1367 (1998) 63–87.

[4] A. Zouni, H. Witt, J. Kern, P. Fromme, N. Krauss, W. Saenger, P. Orth, Crystal structure of photosystem II from *Synechococcus elongatus* at 3.8 Å resolution, Nature 409 (2001) 739–743.

[5] J. Biesiadka, B. Loll, J. Kern, K.D. Irrgang, A. Zouni, Crystal structure of cyanobacterial photosystem II at 3.2 Å resolution: a closer look at the Mn-cluster, Phys. Chem. Chem. Phys. 6 (2004) 4733–4736.

[6] K. Ferreira, T. Iverson, K. Maghlaoui, J. Barber, S. Iwata, Architecture of the photosynthetic oxygen-evolving center, Science 303 (2004) 1831–1838.

[7] A. Guskov, J. Kern, A. Gabdulkhakov, M. Broser, A. Zouni, W. Saenger, Cyanobacterial photosystem II at 2.9-Å resolution and the role of quinones, lipids, channels and chloride, Nat. Struct. Mol. Biol. 16 (2009) 334–342.

[8] J.M. Ortega, M. Hervás, M. Losada, Redox and acid–base characterization of cytochrome *b*-559 in photosystem II particles, Eur. J. Biochem. 171 (1988) 449–455.

[9] O. Kaminskaya, J. Kurreck, K. Irrgang, G. Renger, V. Shuvalov, Redox and spectral properties of cytochrome *b*559 in different preparations of photosystem II, Biochemistry 38 (1999) 16223–16235.

[10] M. Roncel, J.M. Ortega, M. Losada, Factors determining the special redox properties of photosynthetic cytochrome *b*559, Eur. J. Biochem. 268 (2001) 4961–4968.

[11] M. Roncel, A. Boussac, J.L. Zurita, H. Bottin, M. Sugiura, D. Kirilovsky, J.M. Ortega, Redox properties of the photosystem II cytochromes *b*559 and *c*550 in the cyanobacterium *Thermosynechococcus elongatus*, J. Biol. Inorg. Chem. 8 (2003) 206–216.

[12] O. Kaminskaya, V. Shuvalov, G. Renger, Evidence for a novel quinone-binding site in the photosystem II (PSII) complex that regulates the redox potential of cytochrome *b*559, Biochemistry 46 (2007) 1091–1105.

[13] A.C. Stewart, D.S. Bendall, Photosynthetic electron transport in a cell-free preparation from the thermophilic blue-green alga *Phormidium laminosum*, Biochem. J. 188 (1980) 351–361.

[14] Y. Chiu, Y. Chen, M. Roncel, P.L. Dilbeck, J. Huang, K. Shyue-Chu, J.M. Ortega, R.L. Burnap, H. Chu, Spectroscopic and functional characterization of cyanobacterium *Synechocystis* PCC 6803 mutants on the cytoplasmic-side of cytochrome *b*559 in photosystem II, Biochim. Biophys. Acta 1827 (2013) 507–519.

[15] L.K. Thompson, G.W. Brudvig, Cytochrome *b*-559 may function to protect photosystem II from photoinhibition, Biochemistry 27 (1988) 6653–6658.

[16] L. Nedbal, G. Samson, J. Whitmarsh, Redox state of one electron component controls the rate of photoinhibition of Photosystem II, Proc. Natl. Acad. Sci. U. S. A. 89 (1992) 7923–7929.

[17] J. Barber, J. De Las Rivas, A functional model for the role of cytochrome *b*559 in the protection against donor and acceptor side photoinhibition, Proc. Natl. Acad. Sci. U. S. A. 90 (1993) 10942–10946.

[18] J.M. Ortega, M. Hervás, M.A. De la Rosa, M. Losada, pH-dependent photoreactions of the high- and low-potential forms of cytochrome *b*559 in spinach PSII-enriched membranes, Photosynth. Res. 46 (1995) 185–191.

[19] C.A. Tracewell, G.W. Brudvig, Multiple redox-active chlorophylls in the secondary electron-transfer pathways of oxygen-evolving photosystem II, Biochemistry 47 (2008) 11559–11572.

[20] K.E. Shinopoulos, G.W. Brudvig, Cytochrome b_{559} and cyclic electron transfer within photosystem II, Biochim. Biophys. Acta 1817 (2012) 66–75.

[21] J. Kruk, K. Strzalka, Redox changes of cytochrome *b*(559) in the presence of plastoquinones, J. Biol. Chem. 276 (2001) 86–91.

[22] N. Bondarava, C. Gross, M. Mubarakshina, J. Golecki, G. Johnson, A. Krieger-Liszkay, Putative function of cytochrome *b*559 as a plastoquinol oxidase, Physiol. Plant. 138 (2010) 463–473.

[23] N. Bondarava, L. De Pascalis, S. Al-Babili, C. Goussias, J. Golecki, P. Beyer, R. Bock, A. Krieger-Liszkay, Evidence that cytochrome *b*559 mediates the oxidation of reduced plastoquinone in the dark, J. Biol. Chem. 278 (2003) 13554–13560.

[24] A. Tiwari, P. Pospíšil, Superoxide oxidase and reductase activity of cytochrome *b*559 in photosystem II, Biochim. Biophys. Acta 1787 (2009) 985–994.

[25] P. Pospíšil, Enzymatic function of cytochrome *b*559 in photosystem II, J. Photochem. Photobiol. B Biol. 104 (2011) 341–347.

[26] J. Kern, B. Loll, C. Luneberg, D. DiFiore, J. Biesiadka, K.F. Irrgang, A. Zouni, Purification, characterisation and crystallisation of photosystem II from *Thermosynechococcus elongatus* cultivated in a new type of photobioreactor, Biochim. Biophys. Acta 1706 (2005) 147–157.

[27] R. Krivanek, J. Kern, A. Zouni, H. Dau, M. Haumann, Spare quinones in the QB cavity of crystallized photosystem II of *Thermosynechococcus elongatus*, Biochim. Biophys. Acta 1767 (2007) 520–527.

[28] H. Pakrasi, P. De Ciechi, J. Whitmarsh, Site directed mutagenesis of the heme axial ligands of cytochrome *b*559 affects the stability of the photosystem II complex, EMBO J. 10 (1991) 1619–1627.

[29] F. Morais, K. Kühn, D. Stewart, J. Barber, G. Brudvig, P. Nixon, Photosynthetic water oxidation in cytochrome *b*(559) mutants containing a disrupted heme-binding pocket, J. Biol. Chem. 276 (2001) 31986–31993.

[30] F. Morais, J. Barber, P.J. Nixon, The chloroplast-encoded α subunit of cytochrome *b*-559 is required for assembly of the photosystem two complex in both the light and the dark in *Chlamydomonas reinhardtii*, J. Biol. Chem. 273 (1998) 29315–29320.

[31] H. Pakrasi, J. Williams, C. Arntzen, Targeted mutagenesis of the psbE and psbF genes blocks photosynthetic electron transport: evidence for a functional role of cytochrome *b*559 in photosystem II, EMBO J. 7 (1988) 325–332.

[32] C. Hung, J. Huang, Y. Chiu, H. Chu, Site-directed mutagenesis on the heme axial-ligands of cytochrome *b*559 in photosystem II by using cyanobacteria *Synechocystis* PCC 6803, Biochim. Biophys. Acta 1767 (2007) 686–693.

[33] C. Hung, H. Hwang, Y. Chen, Y. Chiu, S. Ke, R. Burnap, H. Chu, Spectroscopic and functional characterizations of cyanobacterium *Synechocystis* PCC 6803 mutants on and near the heme axial ligand of cytochrome *b*559 in photosystem II, J. Biol. Chem. 285 (2010) 5653–5663.

[34] U. Mühlenhoff, F. Chauvat, Gene transfer and manipulation in the thermophilic cyanobacterium *Synechococcus elongatus*, Mol. Gen. Genet. 252 (1996) 93–100.

[35] M. Sugiura, Y. Inoue, Highly purified thermo-stable oxygen-evolving photosystem II core complex from the thermophilic cyanobacterium *Synechococcus elongatus* having His-tagged CP43, Plant Cell Physiol. 40 (1999) 1219–1231.

[36] B. Loll, J. Kern, W. Saenger, A. Zouni, J. Biesiadka, Towards complete cofactor arrangement in the 3.0 Å resolution structure of photosystem II, Nature 438 (2005) 1040–1044.

[37] F. Guerrero, A.I. Sedoud, D. Kirilovsky, A.W. Rutherford, J.M. Ortega, M. Roncel, A high redox potential form of cytochrome c550 in Photosystem II from *Thermosynechococcus elongatus*, J. Biol. Chem. 286 (2011) 5985–5994.

[38] J.W. Golden, D.R. Wiest, Genome rearrangement and nitrogen fixation in *Anabaena* blocked by inactivation of xisA gene, Science 242 (1988) 1421–1423.

[39] D. Kirilovsky, M. Roncel, A. Boussac, A. Wilson, J.L. Zurita, J.M. Ducruet, H. Bottin, M. Sugiura, J.M. Ortega, A.W. Rutherford, Cytochrome *c*550 in the cyanobacterium *Thermosynechococcus elongatus*: study of redox mutants, J. Biol. Chem. 279 (2004) 52869–52880.

[40] Y.P. Cai, C.P. Wolk, Use of a conditionally lethal gene in *Anabaena* sp. strain PCC 7120 to select for double recombination and entrap insertion sequences, J. Bacteriol. 172 (1990) 3138–3145.

[41] T. Miranda, J.M. Ducruet, Characterization of the chlorophyll thermoluminescence afterglow in dark-adapted or far-red-illuminated plant leaves, Plant Physiol. Biochem. 33 (1995) 689–699.

[42] J.M. Ducruet, Chlorophyll thermoluminescence of leaf discs: simple instruments and progress in signal interpretation open the way to new ecophysiological indicators, J. Exp. Bot. 54 (2003) 2419–2430.

[43] J.L. Zurita, M. Roncel, M. Aguilar, J.M. Ortega, A thermoluminescence study of photosystem II back electron transfer reactions in rice leaves. Effects of salt stress, Photosynth. Res. 84 (2005) 131–137.

[44] C. Sajnani, J.L. Zurita, M. Roncel, J.M. Ortega, M. Baron, J.M. Ducruet, Changes in photosynthetic metabolism induced by tobamovirus infection in *Nicotiana benthamiana* studied in vivo by chlorophyll thermoluminescence, New Phytol. 175 (2007) 120–130.

[45] J.M. Ducruet, A. Serrano, M. Roncel, J.M. Ortega, Peculiar properties of chlorophyll thermoluminescence emission of autotrophically or mixotrophically grown *Chlamydomonas reinhardtii*, J. Photochem. Photobiol. B 104 (2011) 301–307.

[46] L.I. Krishtalik, G.S. Tae, D.A. Cherepanov, W.A. Cramer, The redox properties of cytochromes *b* imposed by the membrane electrostatic environment, Biophys. J. 65 (1993) 184–195.

[47] G.S. Tae, M.T. Black, W.A. Cramer, O. Vallon, L. Bogorad, Thylakoid membrane protein topography: transmembrane orientation of the chloroplast cytochrome *b*-559 psbE gene product, Biochemistry 27 (1988) 9075–9080.

[48] F. Guerrero, M. Roncel, D. Kirilovsky, J.M. Ortega, Site-directed mutagenesis of cytochrome *b*559 in the cyanobacterium *Thermosynechococcus elongatus*, in: J.F. Allen, E. Gantt, J.H. Golbeck, B. Osmond (Eds.), Photosynthesis. Energy from the Sun, 14th International Congress on Photosynthesis, Springer, The Netherlands, 2008, pp. 13–16.

[49] A.W. Rutherford, A.R. Crofts, Y. Inoue, Thermoluminescence as a probe of photosystem II photochemistry: the origin of the flash-induced glow peaks, Biochim. Biophys. Acta 682 (1982) 457–465.

[50] I. Vass, Y. Inoue, Thermoluminescence in the study of photosystem II, in: J. Barber (Ed.), Topics in Photosynthesis, The Photosystems: Structure, Function and Molecular BiologyElsevier, Amsterdam, The Netherlands, 1992, pp. 259–294.

[51] Y. Inoue, Photosynthetic thermoluminescence as a simple probe of photosystem II electron transport, in: J. Amesz, A.J. Hoff (Eds.), Biophysical Techniques in Photosynthesis, Kluwer Academic Publishers, The Netherlands, 1996, pp. 93–107.

[52] T. Miranda, J.M. Ducruet, Effects of dark- and light-induced proton gradients in thylakoids on the Q and B thermoluminescence bands, Photosynth. Res. 43 (1995) 251–262.

[53] A.W. Rutherford, Govindje, Y. Inoue, Charge accumulation and photochemistry in leaves studied by thermoluminescence and delayed light emission, Proc. Natl. Acad. Sci. U. S. A. 81 (1984) 1107–1111.

[54] D.V. Vavilin, J.M. Ducruet, The origin of 115–130 °C thermoluminescence bands in chlorophyll-containing material, Photochem. Photobiol. 68 (1998) 191–198.

[55] M. Havaux, K.K. Niyogi, The violaxanthin cycle protects plants from photooxidative damage by more than one mechanism, Proc. Natl. Acad. Sci. U. S. A. 96 (1999) 8762–8767.

[56] D.V. Vavilin, D.N. Matorin, A.B. Rubin, High-temperature thermoluminescence of chlorophyll as a method to study lipid peroxidation in planktonic algae, Arch. Hydrobiol. 153 (2002) 685–701.

[57] J.-M. Ducruet, D. Vavilin, Chlorophyll high-temperature thermoluminescence emission as an indicator of oxidative stress: perturbating effects of oxygen and leaf water, Free Radic. Res. 31 (1999) 187–192.

[58] J. Skotnica, J. Fiala, P. Ilík, L. Dvořák, Thermally induced chemiluminescence of barley leaves, Photochem. Photobiol J. 69 (1999) 211–217.
[59] P. Faller, A. Pascal, A.W. Rutherford, Beta-carotene redox reactions in photosystem II: electron transfer pathway, Biochemistry 40 (2001) 6431–6440.
[60] C.A. Buser, B.A. Diner, G.W. Brudvig, Photooxidation of cytochrome *b*559 in oxygen-evolving photosystem II, Biochemistry 31 (1992) 11449–11459.
[61] R. Bock, H. Kössel, P. Maliga, Introduction of a heterologous editing site into the tobacco plastid genome: the lack of RNA editing leads to a mutant phenotype, EMBO J. 13 (1994) 4623–4628.
[62] A. Prodöhl, T. Volkmer, C. Finger, D. Schneider, Defining the structural basis for assembly of a transmembrane cytochrome, J. Mol. Biol. 350 (2005) 744–756.
[63] R. Gadjieva, F. Mamedov, G. Renger, S. Styring, Interconversion of low- and high-potential forms of cytochrome *b*(559) in Tris-washed photosystem II membranes under aerobic and anaerobic conditions, Biochemistry 38 (1999) 10578–10584.
[64] F. Mamedov, R. Gadjieva, S. Styring, Oxygen-induced changes in the redox state of the cytochrome *b*559 in photosystem II depend on the integrity of the Mn cluster, Physiol. Plant. 131 (2007) 41–49.
[65] J.M. Ortega, M. Hervás, M. Losada, Distinctive stability of the reduced and oxidized forms of high-potential cytochrome *b*-559, Plant Sci. 68 (1990) 71–75.
[66] N. Mizusawa, T. Yamashita, M. Miyao, Restoration of the high-potential form of cytochrome *b*559 of photosystem II occurs via a two-step mechanism under illumination in the presence of manganese ions, Biochim. Biophys. Acta 1410 (1999) 273–286.
[67] P. Pospíšil, A. Tiwari, Differential mechanism of light-induced and oxygen-dependent restoration of the high-potential form of cytochrome *b*(559) in Tris-treated photosystem II membranes, Biochim. Biophys. Acta 1797 (2010) 451–456.
[68] J. Mao, K. Hauser, M. Gunner, How cytochromes with different folds control heme redox potentials, Biochemistry 42 (2003) 9829–9840.
[69] Z. Zheng, M. Gunner, Analysis of the electrochemistry of hemes with E(m)s spanning 800 mV, Proteins 75 (2009) 719–734.
[70] J.-J. Ma, L.-B. Li, Y.-X. Jing, T.-Y. Kuang, Mutation of residue arginine18 of cytochrome *b*559 α-subunit and its effects on photosystem II activities in *Chlamydomonas reinhardtii*, J. Integr. Plant Biol. 49 (2007) 1054–1061.
[71] A. Tiwari, M. Rác, P. Pospíšil, Formation of superoxide anion and carbon-centered radicals by photosystem II under high light and heat stress—EPR spin-trapping study, J. Bioenerg. Biomembr. 45 (2013) 551–559.
[72] F. Rappaport, B.A. Diner, Primary photochemistry and energetics leading to the oxidation of the (Mn)4Ca cluster and to the evolution of molecular oxygen in Photosystem II, Coord. Chem. Rev. 252 (2008) 259–272